Mechanism of carrier accumulation in perovskite thin absorber solar cells

Hui-Seon Kim,[1] Iván Mora-Sero,[*,2] Victoria Gonzalez-Pedro,[2] Francisco Fabregat-Santiago,[2] Emilio J. Juarez-Perez, [2] Nam-Gyu Park,[*,1] and Juan Bisquert[2]

[1] *School of Chemical Engineering and Department of Energy Science, Sungkyunkwan University, Suwon 440-746, Korea*

[2] *Photovoltaic and Optoelectronic Devices Group, Departament de Física, Universitat Jaume I, 12071 Castelló, Spain.*

[*]Corresponding Authors: sero@fca.uji.es, npark@skku.edu,

Abstract

Photovoltaic conversion requires two successive steps: accumulation of photogenerated charge and charge separation. Determination of how and where charge accumulation is attained and how this accumulation can be identified, is mandatory to understand the performance of a photovoltaic device and to develop its further optimization. Here we analyze the mechanism of carrier accumulation in lead halide perovskite, $CH_3NH_3PbI_3$, thin absorber solar cells by impedance spectroscopy (IS). A fingerprint of the charge accumulation in high density of states of the perovskite absorber material has been observed at the capacitance of the samples. This is, as far as we know, the first observation of charge accumulation in the light absorbing material for nanostructured solar cells, indicating that it constitutes a new kind of photovoltaic device, differentiated from sensitized solar cells, that will require its own methods of study, characterization and optimization.

Nanostructured solar cells constitute a powerful alternative for the development of the third generation of photovoltaic devices. The second generation, thin film solar cells, allows in many cases a reduction of production cost in comparison with first generation, Si solar cells. In the third generation, in addition, an increase of the efficiencies is potentially attainable.[1] To reduce the cost of the photovoltaic devices, an efficient strategy is to relax the quality requirements of the materials forming the device. But in conventional Si solar cells high crystal quality is required, as both photogenerated electrons and holes are transported along the same material and defects act as recombination centers reducing the cell performance. The material quality can be relaxed if just one carrier is transported along one specific material. This is the working principle of sensitized solar cells (SSCs) where light absorption and carrier transport are decoupled.[2] In sensitized solar cells, charge is photogenerated in dye (DSSCs), thin semiconductor (SSSCs) or in a semiconductor quantum dot (QDSSCs), for small semiconductor nanocrystal sensitizers where the regime of quantum confinement is reached.[3,4] The photogenerated charge is quickly injected into two different transport media (TM). One for electrons (ETM), generally a wide band gap semiconductor as TiO_2, and the other one for holes (HTM). As only a single carrier is present in the transporting media, the carrier recombination is reduced and less demanding materials can be employed. In this context, the necessity of nanostructured devices arises from the fact that a single molecular layer or semiconductor extremely thin absorber (~nm) cannot completely harvest the incident sunlight. By nanostructuring the electrode, the effective area to be covered by the sensitizer can be increased by several orders of magnitude. In fact the appearance of these electrodes enormously

increased the efficiency of DSSCs.[2] In this sense, the role of nanostructured metal oxide electrodes is well defined as selective electron contact and ETM with high effective surface area to enhance cell harvesting.

Since the seminal paper on DSSCs of O'Regan and Grätzel in the early 1990s[2], the recent demonstration of all-solid nanostructured solar cells with efficiency higher than 10% constitutes one of the most important breakthroughs in this field.[5-8] Open circuit voltages as high as 1.3 V (ref. [9]) and efficiencies of 12.3%,[7,8] even higher than the record liquid DSSC, have been very recently demonstrated. In this kind of cell, nanoparticles or thin film of $CH_3NH_3PbX_3$, with perovskite crystalline structure (where X is a halogen element I, Cl, Br or a combination), are deposited on a nanostructured semiconductor with or without hole transporting material (HTM). Lead halide perovskites have already shown a great potential in QDSSCs with a liquid HTM.[10,11] However, it was the recent reports on all-solid devices, with easier perspectives for industrialization, that has revolutionized the field of nanostructured photovoltaic devices. However, the working principles of these devices are not completely understood as there are clear evidences that these devices do not work as the conventional sensitized solar cell, where both ETM and HTM are needed. Solar cells with lead halide perovskite and no ETM have been prepared with η=10.9% using Al_2O_3 nanostructured electrode in which perovskite cannot photoinject due to a type I band alignment,[6] while devices with no HTM and η=5.5%, have been prepared contacting directly the perovskite with an Au contact.[12]

In this work, to unveil the working principles of these devices, and concretely understand the mechanism of charge accumulation needed for the

photovoltaic conversion, a systematic study based on impedance spectroscopy (IS) characterization has been carried out, under dark and under illumination conditions. The direct signature of perovskite light absorbing material has been observed in the capacitance of the device, indicating charge accumulation in the electronic states of perovskite. In the DSSC the charge accumulation in the light absorbing material (the dye) has not been detected by electrochemical measurement, and for QDSSCs it was detected indirectly as a change in the capacitance slope.[13] Here we present the first report of charge accumulation in the light absorbing material for nanostructured solar cells, which is attributed to a density of states (DOS) that is larger in the perovskite absorber than in either ETM or HTM. This fact makes lead halide perovskite solar cells a new type of photovoltaic device halfway between nanostructured and thin-film solar cells.

Results

Performance of flat and nanostructured solar cells

In order to have a general view of the performance of photovoltaic devices using perovskite as light absorbing material, different cells with flat and nanostructured (NS) electrodes have been prepared using $CH_3NH_3PbI_3$ as light absorbing material. $CH_3NH_3PbI_3$ was prepared following the previously reported methods.[5] Briefly, glass covered with a thin-film of transparent conductive SnO_2:F (FTO) was used as substrate for electrode preparation. A compact layer of TiO_2 was deposited on top of FTO. Electrodes prepared in this way are called hereafter "Flat" electrodes. Two types of NS electrodes were prepared with an additional layer formed by TiO_2 or ZrO_2 nanoparticles. Finally on these electrodes are sequentially deposited

$CH_3NH_3PbI_3$, spiro-MeOTAD as HTM and Au contact. SEM, TEM and energy dispersive X-ray spectroscopy (EDXS) characterization of Flat and NS devices can be found in Supplementary Figures S1, S2, S3 and S4. Blank cells prepared exactly in the same way but without perovskite have been also prepared. See Methods section for more details about sample preparation.

Fig. 1 shows the current-potential (J-V) curves of samples prepared with the different electrodes at 1 sun illumination. The solar cell parameters, components and geometrical issues of these samples are reported in Table 1. All the prepared devices exhibit high open circuit potential, V_{OC}. The photocurrent, J_{SC}, obtained decreases from NS TiO_2 to NS ZrO_2 to Flat electrode. The light absorption measured for NS ZrO_2 with perovskite electrodes is lower than for NS TiO_2 electrodes of the same thickness, see Supplementary Figure S5. Cell prepared with NS TiO_2 also exhibits higher FF and consequently the highest conversion efficiency of the set, a significant η=7.8%. Sample prepared on NS ZrO_2 electrode presents an appreciable efficiency of 4.2%. It is also interesting to point out that non negligible efficiency and photocurrent is obtained even for Flat device, as it has been already seen for other inorganic semiconductors[14] but not for dyes,[15] due to the high perovskite extinction coefficient. In Supplementary Figure S6 the results obtained in this work for NS and flat samples are compared with our previous report on all-solid quantum dot sensitized solar cells of TiO_2/Sb_2S_3/P3HT (ref. [14]) in order to highlight the consistence of both results.

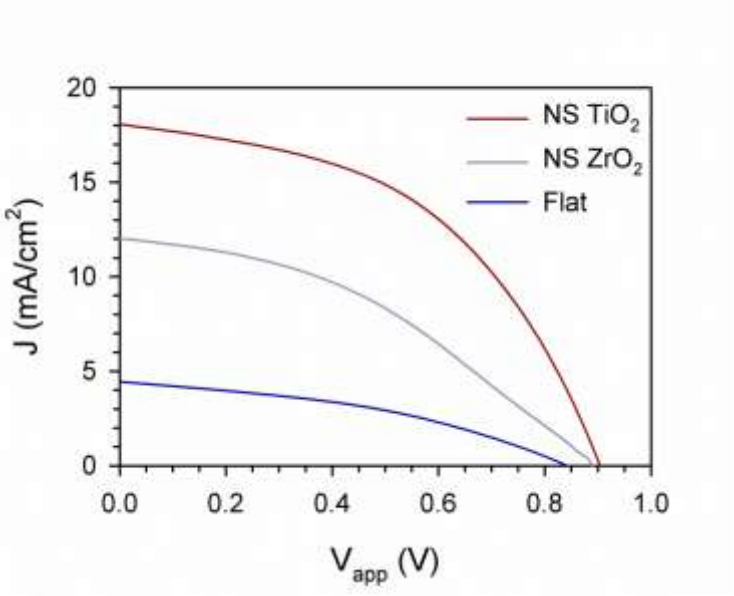

Figure 1: Solar Cell Performance. Current potential J-V curves of lead iodine perovskite with three different electrodes: FTO/Compact TiO_2 (Flat), FTO/Compact TiO_2/Nanoestructured TiO_2 (NS TiO_2) and FTO/Compact TiO_2/Nanoestructured ZrO_2 (NS ZrO_2). Solar cell parameters and conversion efficiency are summarized in Table 1.

Table 1: Solar Cell Parameters. Structure, material, thickness, area and solar cell parameters of the devices analyzed in Fig. 1. The solar cell parameters indicated are short circuit current, J_{SC}, open circuit voltage, V_{OC}, fill factor, FF, and photoconversion efficiency, η.

Compact layer /nanostructured film	Thickness nanostructured film (μm)	Area (cm^2)	J_{SC} (mA/cm^2)	V_{OC} (mV)	FF	η (%)
TiO_2 / -	0	0.180	4.4	841	0.39	1.5
TiO_2 / ZrO_2	0.36	0.195	12.0	899	0.39	4.2
TiO_2 / TiO_2	0.55	0.195	18.1	903	0.48	7.8

The conduction band (CB) of $CH_3NH_3PbI_3$ is situated at -3.93 eV vs. vacuum while TiO_2 is situated around -4 eV as it has been determined by ultraviolet

photoelectron spectroscopy (UPS).[5] Therefore photogenerated charge in $CH_3NH_3PbI_3$ perovskite can potentially be injected into TiO_2 as there exists an adequate band alignment. This is not the case for ZrO_2 with a CB 0.82 eV higher than the CB of TiO_2.[16] ZrO_2 is commonly used as control measurement for the characterization of sensitizers as no injection into ZrO_2 is observed, in contrast with TiO_2.[17] In fact no photovoltaic performance was observed for samples prepared with compact ZrO_2 layer instead of compact TiO_2, as we have verified experimentally.

The electrical differences between TiO_2 and ZrO_2 electrodes have been investigated by three electrode electrochemical measurements using a liquid electrolyte. Liquid electrolytes are excellent contacts for nanostructured samples as liquid wets all the NS surface. Moreover, through the utilization of a redox couple the Fermi level at the solution can be fixed, and all the observed voltage drop is at the semiconductor electrode side. Fig. 2 shows the capacitance of different electrodes formed with a compact layer and a nanoporous layer of TiO_2 and ZrO_2. It can be observed that the capacitance of bare FTO layer presents only a slight variation as function of the applied voltage, V_{app}. Similar behaviour is observed for the electrode with ZrO_2 compact layer (ZZ) and with nanoporous ZrO_2 layer but no compact layer (0Z)). Thus, NS ZrO_2 layers are not charged with the applied bias. Moreover, at high V_{app} an exponential increase of capacitance is observed for the electrode with only TiO_2 compact layer (T0), corresponding to the chemical capacitance of the compact TiO_2.[18,19] The increase of capacitance is higher for the electrode with also NS layer of TiO_2 (TT) due to the higher TiO_2 volume than T0 electrode. Contrary to ZrO_2, TiO_2 can be charged. The chemical capacitance pattern reflects the exponential TiO_2 Density Of States (DOS). [18,19] As the V_{app} is

increased, charge is accumulated in the TiO_2 DOS while not in ZrO_2. Only when TiO_2 compact layer is used with ZrO_2 nonporous electrode (TZ) exponential increase of the chemical capacitance can be observed, corresponding to the chemical capacitance of TiO_2 compact layer, as can be inferred from the results in Fig. 2. This analysis gives an additional proof that no charge is accumulated into ZrO_2. In this case, ZrO_2 is acting as scaffold for perovskite as Al_2O_3 in a previous reports.[6,9]

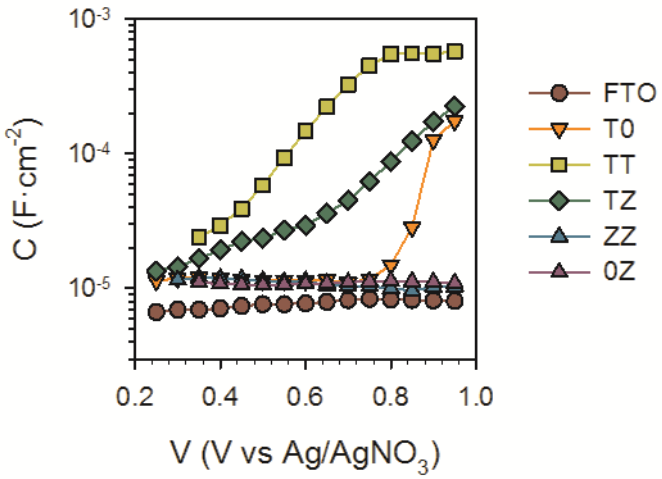

Figure 2: Capacitance of non-sensitized electrodes. Capacitance has been extracted from IS measurements in liquid electrolyte with I^-/I^{3-} redox couple. Capacitance of bare conductive Sn_2O:F (FTO) electrode is compared with electrodes with up to different layers of TiO_2 and ZrO_2. The electrodes are called using the notation XY, where X is a compact layer and Y a porous layer, T and Z mean TiO_2 and ZrO_2 layer respectively. 0 means no layer i.e. T0 compact TiO_2 layer with no nanoporous layer.

Impedance spectroscopy interpretation

Just from J-V curves it is difficult to extract conclusions about the mechanism that determines the different behavior observed among the different electrodes analyzed. It is not straightforward, and many times impossible, to decouple the

effect on J-V curve of each part of the device, only with this characterization. Nevertheless Impedance Spectroscopy (IS) is a frequency characterization technique that allows to decouple physical processes with different characteristic times.[19] Its interpretation is not trivial, but once the appropriate models are developed this technique allows separate characterization of each part of the full device at the cell working conditions. We have employed this method to analyze the prepared solar cells under dark and 1 sun illumination conditions. Here we have focused in the determination of charge accumulation, strictly needed for the photovoltaic process. The detailed analysis of all aspects of the impedance spectra, is beyond the scope of this communication. Nevertheless we have developed an advanced model that allows to extract all the relevant information from the impedance spectra, taking in consideration some previous results on DSSCs.[20] All details on the IS model employed for the characterization of the measured samples can be found in Supplementary Note 1.

Fig. 3 shows an example of the Nyquist plots obtained for the analyzed cells. The results correspond to NS TiO_2 and ZrO_2 solar cell under dark and under illumination, both at V_{app} =0 and 0.8 V. The first remarkable fact is that, in spite of the clear differences between TiO_2 and ZrO_2 electrodes, discussed previously as regard of Fig. 2, similar impedance patterns are obtained for both electrodes. It is also significant the apparition of a transmission line (TL) under dark and low V_{app} conditions, characterized by a straight line followed by an arc, see Fig. 3a and 3b. TL is the classical feature obtained for nanostructured electrodes where transport is coupled with recombination,[21] see Supplementary Figure S9. But in the case of NS TiO_2 electrodes usually is not possible to observe it for very thin electrodes, as in the case of Fig. 3, see Table 1, and at least electrodes thicker than 2-3 μm are

needed to appreciate this feature. These two facts are indicating that new

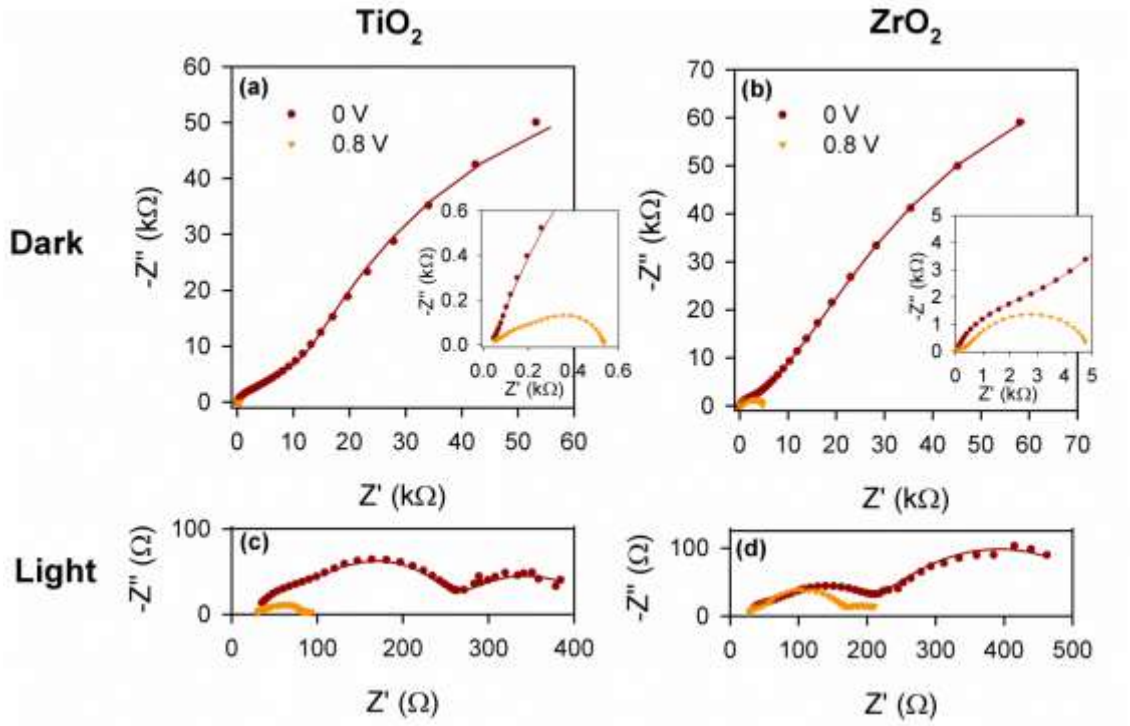

behaviors, in comparison with conventional sensitized solar cells, can be attributed to NS perovskite solar cells.

Figure 3: Nyquist plots of lead iodine perovskite solar cells in TiO_2 and ZrO_2 electrodes. Nyquist plot of solar cell prepared in the form FTO/Compact TiO_2/Nanostructured Oxide/Perovskite/spiro-MeOTAD/Au. Left column correspond to the device using TiO_2 as nanostructured oxide, while right column to device with ZrO_2, shown in Fig. 1 and summarized in Table 1. (a) and (b) correspond to IS measurements under dark conditions transmission line behavior is clearly visible. The inset is a zoom of the low impedance region. (c) and (d) correspond to measurements under 1 sun illumination. Nyquist plots for two different applied DC signal, V_{app}, are shown in the graphs. Solid lines are the fits obtained using equivalent circuits previously used for solid DSSC with spiro-MeOTAD,[22] and in some cases additional R-C feature to the TL for an accurate fitting, see Supplementary Figure S9.

The capacitance and the density of states

The direct finger print of charge accumulation should be observed in the capacitance as chemical capacitance reflects the capability of a system to accept or release additional carriers due to a change in its Fermi level.[18] The Nyquist plots in Fig. 3 present a rich impedance pattern with several features. It is not straightforward to determine in which part of IS spectra is contained the information about chemical capacitance, see Supplementary Note 1 for further discussions. IS spectra has been fitted using equivalent circuits previously used for solid DSSC with spiro-MeOTAD.[22] The use of spiro-MeOTAD as HTM adds an extra degree of complexity in the analysis as it has been pointed out recently,[23] and in some cases it introduces an additional R-C feature to the TL circuit. Focusing in the spectra under illumination conditions, Fig. 3c and d, three regions can be discriminated, at high, intermediate and low frequencies, called hereafter *hf*, *if* and *lf*, respectively. Taking into consideration these features, capacitance of different electrodes has been determined from *if* region, see Supplementary Note 1.

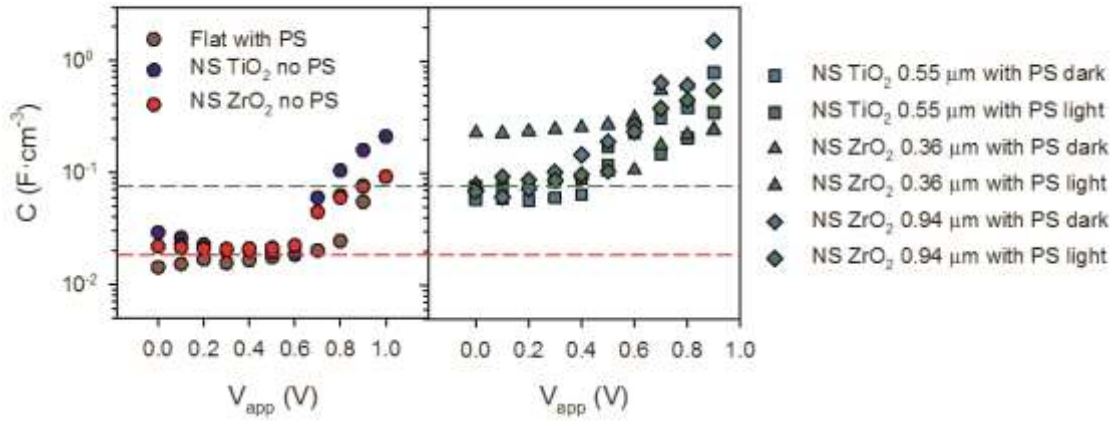

Figure 4: Capacitance analysis of flat samples and NS samples with and without perovskite. Left graph plots capacitance of flat with perovskite (PS) and blank samples without PS, NS TiO_2 and ZrO_2 samples present NS layers of 0.35 µm

TiO_2 and 0.39 μm ZrO_2 respectively. Right graph plots the capacitance of NS TiO_2 and ZrO_2 samples with perovskite of samples with different NS layer thickness as it is indicated in the legend. Capacitance obtained in measurements under dark and under 1 sun illumination (light) conditions are plotted. Capacitance for both graphs has been extracted by fitting the IS spectra from the *if* region as discussed in Supplementary Note 1. Capacitance has been normalized to the electrode volume. Red and green dashed lines and only eye guides to highlight the difference in capacitance obtained for samples with and without perovskite.

From the general knowledge of IS analysis of DSSC, it is well established that the compact layer generally used to cover the conducting glass, has a large effect on the capacitance, when the interface is polarized at reverse or moderate forward bias. It is therefore important to analyze such layer using the Flat samples in order to separately determine the capacitance contribution of NS layers which are the active photovoltaic layers. Fig. 4 shows the capacitance extracted from IS spectra fitting, for Flat and NS samples, with and without perovskite, for both TiO_2 and ZrO_2 electrodes. The left graph includes Flat and blank NS samples (without perovskite) while right graph includes NS solar cells with perovskite. In the left graph of Fig. 4, two regions, independently of the NS film material, can be appreciated. One at low V_{app}, V_{app} <0.6-0.7 V, and the other one at high V_{app}. For Flat sample at low V_{app} the growth of capacitance with the voltage is moderate and in Fig. 4 it is appreciated as practically constant with the logarithmic scale employed in the representation, see red dashed line used as eye guide. At high V_{app} an increase on the capacitance slope is observed. This exponential enhancement of capacitance can be attributed to the chemical capacitance of flat TiO_2 compact layer, as it has been pointed out in Fig. 2 for T0 electrode with only TiO_2 compact layer. Moreover, the less voltage dependent capacitance at low V_{app} could be

related with the capacitance of the spiro-MeOTAD with some contribution from the interface capacitance at compact TiO_2/spiro-MeOTAD.[24] We consider that the role of perovskite in this capacitance is minor (just reducing the compact TiO_2/spiro-MeOTAD interface effective area) as the amount of perovskite involved is minimal. Confirming this aspect, it is observed a similar behavior for perovskite free (blank) NS samples independently of the NS layer material TiO_2 or ZrO_2. For blank NS samples an increase of capacitance at high V_{app} is also observed, and it is more significant for NS TiO_2 as in this case the chemical capacitance of the NS TiO_2 layer also participates, as it has been discussed in Fig. 2. Note that with the experimental procedure reported in the Methods section for the preparation of $CH_3NH_3PbI_3$ the amount of perovskite deposited in Flat sample is low and it is not enough to produce a distinguishable continuous thin layer of perovskite as can be observed in SEM pictures in Supplementary Figure S3. This fact prevented the investigation of the capacitance of thicker $CH_3NH_3PbI_3$ layers.

In the case of complete NS devices with perovskite, right graph Fig. 4, a clear difference in the capacitance value is observed, obtaining higher capacitances for samples with perovskite than for blank samples, see red and green dashed lines in Fig. 4. It is worth to point out that the normalized capacitance is independent of the electrode material (TiO_2 or ZrO_2), the NS layer thickness and the illumination conditions at which the IS characterization was carried out (only NS ZrO_2, 0.35 μm thickness, under dark separates from the general trend at low V_{app}). This observation indicates that the capacitance, observed in this case, is neither the interfacial resistance at the compact TiO_2 interface nor the spiro-MeOTAD nor the TiO_2 (compact or NS) chemical capacitance, or at least not only the TiO_2 chemical capacitance as similar behavior is observed in ZrO_2 samples. The remaining

possibility is that this capacitance is originated by the perovskite deposited in the NS layer. Charge accumulation in perovskite material is directly observed. As chemical capacitance maps the DOS, the high perovskite capacitance indicates a high DOS density in this material. This is as far as we know the first observation of charge accumulation in the light absorbing material for nanostructured solar cells using a combination of absorber, ETM and HTM. This conclusion is supported also by the observation of a large capacitance in Flat sample with a thin film of perovskite, further described below..

In order to highlight this new feature observed in NS perovskite solar cells, classical all-solid DSSC with dye N719 and spiro-MeOTAD as HTM has been prepared and characterized, see Supplementary Figures S10 and S11.

The comparison of the capacitance observed for DSSC and the other samples (with NS TiO_2 or ZrO_2) analyzed here is displayed in Fig. 5. It is well known that the chemical capacitance extracted from DSSC is the chemical capacitance of the NS TiO_2 layer.[18,19,22] Chemical capacitance of DSSC, obtained from *if* region, represented with inverted triangles with red edge in Fig. 5 reflects the exponential DOS of TiO_2. Note the significant difference between the chemical capacitance of DSSC and NS TiO_2 perovskite solar cell (consider only the capacitance extracted at *if* region). Only at high V_{app} both capacitances merge indicating a possible contribution of both materials, perovskite and NS TiO_2, to the charge accumulation. In the case for NS ZrO_2 samples with perovskite, the main contribution to the capacitance is from perovskite but a contribution of compact TiO_2 cannot be ruled out at high V_{app}. These results indicate that although sensitized solar cells and perovskite NS solar cells presents similar configuration

(when NS TiO_2 electrode is used) the working principles are different with charge accumulation and transport in perovskite material exhibiting a very large DOS. Deep knowledge of these working principles of perovskite NS solar cells is mandatory for a further improvement of this new kind of devices.

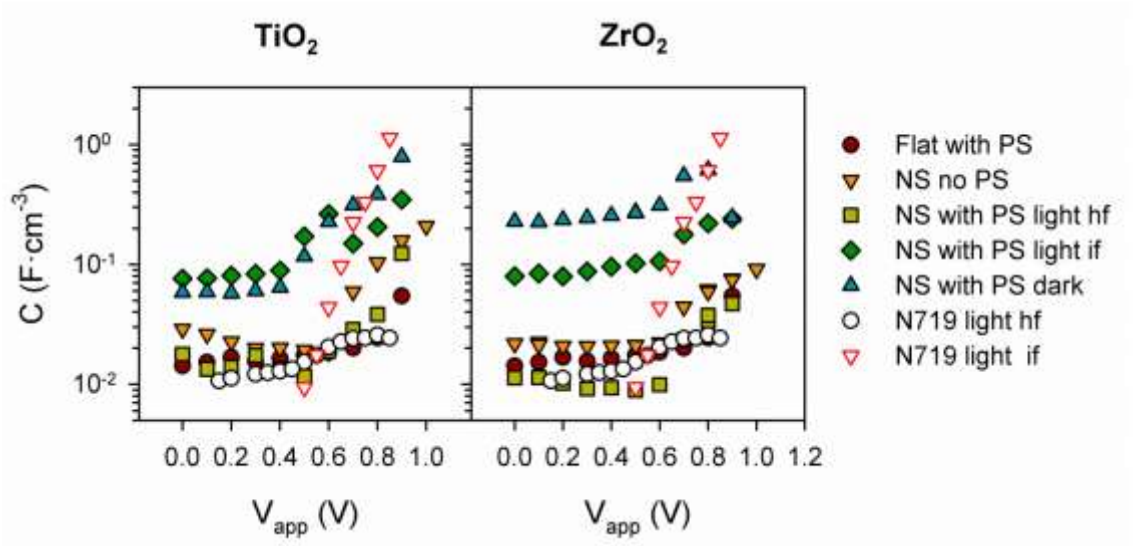

Figure 5: Capacitance analysis of TiO_2 and ZrO_2 and comparison with a solid DSSC using N719 dye. Left graph plots capacitance of: flat sample with perovskite (PS); blank NS TiO_2 (0.35 µm thickness) with no PS; NS TiO_2 (0.55 µm thickness) with PS extracted from measurement under dark and under 1 sun illumination (light) conditions; and all-solid DSSC (2.2 µm thickness) with N719 as dye and spiro-MeOTAD as HTM. Right graph plots capacitance offlat sample with perovskite (PS); blank NS ZrO_2 (0.39 µm thickness) with no PS; NS TiO_2 (0.36 µm thickness) with PS extracted from measurement under dark and under 1 sun illumination (light) conditions; and all-solid DSSC (2.2 µm thickness) with N719 as dye and spiro-MeOTAD as HTM. Capacitance has been normalized to the electrode volume. Capacitance for both graphs has been extracted by fitting the IS spectra from the *if* region if nothing else is indicated. In some cases capacitance has been extracted from the *hf* region as it is indicated in the legend.

Thin film solar cell

Since the results reported so far in the literature indicate that the organometal halide perovskite may work both as light absorber and as ambipolar electron and hole transport material, it is of great interest to explore the operation of these materials in thin film solar cell configuration, in which a compact layer is sandwiched between selective contacts. It is important, therefore, to confirm that the distinctive large DOS observed in nanostructured samples is found as well in planar samples. We have commented above on very thin layers of $CH_3NH_3PbI_3$ but the capacitance results were not conclusive. Therefore we have also prepared a Flat cell of $CH_3NH_3PbI_{3-x}Cl_x$ following a processing method recently reported,[8] obtaining a Flat sample with a perovskite layer of 300 nm. The measurements of capacitance of such thin film configuration, described in Supplementary Note 2, indicate a large capacitance that doubtless corresponds to the perovskite layer, see Supplementary Figure S13, confirming our results above for nanostructured perovskite samples about the huge intrinsic DOS of this type of materials.

Discussion

In this Article we showed for the first time the charge accumulation in the light absorbing materials, $CH_3NH_3PbI_3$ perovskite, in a nanostructured solar cell. High DOS has been observed for perovskite. This direct evidence has been observed by the capacitance extracted from IS measurements for both NS TiO_2 or ZrO_2 electrodes, in spite of the large differences from the electrical point of view between these two materials. This study indicates that the analyzed solar cell constitutes a new kind of photovoltaic device halfway between sensitized and thin-film solar cell for NS TiO_2 and a thin-film solar cell with ZrO_2 scaffold for NS ZrO_2.

The optimization and further improvement of a new photovoltaic technology requires of a deep knowledge of the working principles of this photovoltaic device. Understanding how charge accumulation is reached and how it can be identified and characterized is an important step forward in this direction, with significant implications in the development of this technology.

Methods

Electrode preparation and characterization. The electrodes analyzed in this study include flat and nanoporous morphologies for TiO_2 and ZrO_2. The semiconductor compact layers (CL) were prepared by spin coating on Fluorine-doped Tin Oxide (FTO) covered glass substrates (Pilkington TEC 15) a solution of M (IV) bis(ethyl acetoacetato)-diisopropoxide (M = Ti or Zr) 0.15 M in 1-butanol. The coated films were cooled down, and the spin–cast was repeated twice with a double concentrated precursor solution followed by a thermal treatment at 450 ºC. The thicknesses determined by Scanning Electron Microscopy were ~100 nm and ~60 nm for TiO_2 and ZrO_2, respectively. Porous TiO_2 film was prepared by doctor blade method using 20 nm sized paste prepared according to the method described elsewhere[25] and sintering at 450 ºC for 30 min in air. Porous ZrO_2 film was also prepared by doctor blade method using ZrO_2 paste with a particle size of 15 nm[25] and sintered under the same condition with porous TiO_2 film. The thicknesses of nanoporous films were ~ 0.3-2 μm for solar cell characterization and 2-4 μm for electrode characterization. $CH_3NH_3PbI_3$ perovskite precursor solution was prepared by mixing PbI_2 (1.23 mmol, 99%, Aldrich) and CH_3NH_3I (1.23 mmol, synthesized) in γ-butyrolactone (1 mL, 99%, Fluka) producing 40 wt.% solution. The CH_3NH_3I was readily synthesized by reacting CH_3NH_2 (0.273 mol, 40% in methanol, TCI) with HI (0.227 mol, 57 wt.% in water, Aldrich) according to the method reported elsewhere.[5,10] The perovskite precursor solution kept at 60 ^oC with stirring for 12 hr was deposited on the prepared flat or nanoporous TiO_2 and ZrO_2 films by spin-coating process, which was followed by heating at 100 ^oC for 15 min. The perovskite-adsorbed films were covered with hole transport material

(HTM) using spin-coating method, where HTM solution is composed of 0.14 M 2,2',7,7'-tetrakis-(N,N-di-*p*-methoxyphenyl-amine)-9,9'-spirobifluorene (spiro-MeOTAD, Merck), 64 mM bis(trifluoromethane)sulfonamide lithium salt (Li-TFSI, 99.95%, Aldrich), and 0.198 M 4-*tert*-butylpyridine (*t*BP, 96%, Aldrich) in the mixture of chlorobenzene (99.8%, Aldrich) and acetonitrile (99.8%, Aldrich) with a volume ratio of 10:1. A 70 nm-thick Au (99.99%) layer as a counter electrode was evaporated on the top of the HTM overlayer under ca. 10^{-6} mbar. J-V characteristics of QDSCs were performed under 1 sun illumination (AM 1.5 G, 100 $mWcm^{-2}$) with an ABET Sun 2000 solar simulator (1000W Xe source) and a Keithley 2400 source meter. Measurements were carried out without mask. This procedure overestimates the efficiency ~10%.[26] Photoelectrochemical measurements were performed using a FRA-equipped PGSTAT-30 from Autolab. A three electrode configuration was used where a Pt wire was connected as counterelectrode and Ag/Ag^{+} non-aqueous as reference electrode. Anhydrous and degassed acetonitrile with redox iodide/triiodide (0.5 M LiI, 0.05 M I_2) was used as electrolyte. Cyclic voltametries were recorded at a scan rate of 50 mV/s and impedance characterization was performed at forward bias, applying a 20mV AC sinusoidal signal over the constant applied bias with the frequency ranging between 400 kHz and 0.1 Hz.

Acknowledgements

We thank the following agencies for support of this research: Ministerio de Educacion y Ciencia under project HOPE CSD2007-00007, Generalitat Valenciana (ISIC/2012/008) and Universitat Jaume I project 12I361.01/1. This work was also supported by the National Research Foundation of Korea (NRF) grant funded by the Ministry of Science, ICT & Future Planning (MSIP) of Korea under contracts No. NRF-2012M1A2A2671721, NRF-2010-0014992, and NRF-2012M3A6A7054861 (the Global Frontier R&D Program on Center for Multiscale Energy System). H.S.K. was grateful for the global Ph. D. fellowship grant funded by NRF (NRF-2011-0008467). We thank Mr. Dae-Yong Son for preparation of ZrO_2 paste. We thank Prof. A. Maquieira and Dr. M.J. Bañuls from the Institute of Molecular Recognition and Technological Development (Polytechnic University of Valencia), for SEM measurements of $CH_3NH_3PbI_{3-x}Cl_x$ samples.

Author contributions

H.S.K. prepared the samples and perform the characterization for most of the analyzed samples, V.G.P. prepared and characterized the remaining samples, E.J.J.P. prepared and characterized Flat $CH_3NH_3PbI_{3-x}Cl_x$ samples, J.B., F.F.S. and I.M.S. design the experiments, H.S.K., F.F.S. and I.M.S. analyzed the data, N.G.P. and J.B. directed this study, I.M.S. wrote the first version of the manuscript, all authors discussed the results and contributed to the final version of the paper.

Additional information

Supplementary Information accompanies this paper at

http://www.nature.com/naturecommunications

Competing financial interests: The authors declare no competing financial interests.

Reprints and permission information is available online at

http://npg.nature.com/reprintsandpermissions/

References

1 Nozik, A. J. Quantum Dot Solar Cells. *Physica E* **14**, 115-200 (2002).

2 O'Regan, B. & Gratzel, M. A Low-Cost, High-Efficiency Solar-Cell Based on Dye-Sensitized Colloidal TiO2 Films. *Nature* **353**, 737-740 (1991).

3 Hodes, G. Comparison of Dye- and Semiconductor-Sensitized Porous Nanocrystalline Liquid Junction Solar Cells. *J. Phys. Chem. C* **112**, 17778-17787 (2008).

4 Mora-Seró, I. & Bisquert , J. Breakthroughs in the Development of Semiconductor-Sensitized Solar Cells. *J. Phys. Chem. Lett.* **1**, 3046–3052 (2010).

5 Kim, H.-S. *et al.* Lead Iodide Perovskite Sensitized All-Solid-State Submicron Thin Film Mesoscopic Solar Cell with Efficiency Exceeding 9%. *Sci. Rep.* **2**, 591 (2012).

6 Lee, M. M., Teuscher, J., Miyasaka, T., Murakami, T. N. & Snaith, H. J. Efficient Hybrid Solar Cells Based on Meso-Superstructured Organometal Halide Perovskites. *Science* **338**, 643-647 (2012).

7 Noh, J. H., Im, S. H., Heo, J. H., Mandal, T. N. & Seok, S. I. Chemical Management for Colorful, Efficient, and Stable Inorganic–Organic Hybrid Nanostructured Solar Cells. *Nano Letters***13**, 1764-1769 (2013).

8 Ball, J. M., Lee, M. M., Hey, A. & Snaith, H. Low-Temperature Processed Mesosuperstructured to Thin-Film Perovskite Solar Cells. *Energy & Environmental Science* **6**, 1739-1743 (2013).

9 Edri, E., Kirmayer, S., Cahen, D. & Hodes, G. High Open-Circuit Voltage Solar Cells Based on Organic–Inorganic Lead Bromide Perovskite. *J. Chem. Phys. Lett.* **4**, 897-902 (2013).

10 Im, J.-H., Lee, C.-R., Lee, J.-W., Park, S.-W. & Park, N.-G. 6.5% efficient perovskite quantum-dot-sensitized solar cell. *Nanoscale* **3**, 4088-4093 (2011).

11 Kojima, A., Teshima, K., Shirai, Y. & Miyasaka, T. Organometal Halide Perovskites as Visible-Light Sensitizers for Photovoltaic Cells. *J. Am. Chem. Soc.* **131**, 6050-6051 (2009).

12 Etgar, L. *et al.* Mesoscopic CH3NH3PbI3/TiO2 Heterojunction Solar Cells. *J. Am. Chem. Soc.* **134**, 17396-17399 (2012).

13 Hod, I. *et al.* Dye versus Quantum Dots in Sensitized Solar Cells: Participation of Quantum Dot Absorber in the Recombination Process. *J. Phys. Chem. Lett.* **2**, 3032–3035 (2011).

14 Boix, P. P. *et al.* From Flat to Nanostructured Photovoltaics: Balance between Thickness of the Absorber and Charge Screening in Sensitized Solar Cells. *ACS Nano* **6**, 873–880 (2012).

15 Unger, E. L. *et al.* Bilayer Hybrid Solar Cells Based on Triphenylamine-Thienylenevinylene Dye and TiO_2. *J. Phys. Chem. C* **114**, 11659–11664 (2010).

16 Palomares, E., Clifford, J. N., Haque, S. A., Lutz, T. & Durrant, J. R. Control of Charge Recombination Dynamics in Dye Sensitized Solar Cells by the Use of Conformally Deposited Metal Oxide Blocking Layers. *Journal of the American Chemical Society* **125**, 475-482 (2003).

17 Topoglidis, E., Campbell, C. J., Palomares, E. & Durrant, J. R. Photoelectrochemical study of Zn cytochrome-c immobilised on a nanoporous metal oxide electrode. *Chem. Comm.* **0**, 1518-1519 (2002).

18 Bisquert, J. Chemical capacitance of nanostructured semiconductors: its origin and significance for nanocomposite solar cells. *Phys. Chem. Chem. Phys.* **5**, 5360-5364 (2003).

19 Fabregat-Santiago, F., Garcia-Belmonte, G., Mora-Seró, I. & Bisquert, J. Characterization of nanostructured hybrid and organic solar cells by impedance spectroscopy. *Phys. Chem. Chem. Phys.* **13**, 9083–9118 (2011).

20 Bisquert, J., Grätzel, M., Wang, Q. & Fabregat-Santiago, F. Three-Channel Transmission Line Impedance Model for Mesoscopic Oxide Electrodes Functionalized with a Conductive Coating. *J. Chem. Phys. B* **110**, 11284-11290 (2006).

21 Bisquert, J. Theory of the Impedance of Electron Diffusion and Recombination in a Thin Layer. *J. Chem. Phys. B* **106**, 325-333 (2002).

22 Fabregat-Santiago, F. *et al.* Electron Transport and Recombination in Solid-State Dye Solar Cell with Spiro-OMeTAD as Hole Conductor. *J. Am. Chem. Soc.* **131**, 558-562 (2009).

23 Dualeh, A., Moehl, T., Nazeeruddin, M. K. & Grätzel, M. Temperature Dependence of Transport Properties of Spiro-MeOTAD as a Hole Transport Material in Solid-State Dye-Sensitized Solar Cells. *ACS Nano* **7**, 2292-2301 (2013).

24 Fabregat-Santiago, F., Garcia-Belmonte, G., Bisquert, J., Bogdanoff, P. & Zaban, A. Mott-Schottky analysis of nanoporous semiconductor electrodes in the dielectric state deposited on SnO2(F) conducting substrates. *Journal of the Electrochemical Society* **150**, E293-E298 (2002).

25 Kim, M.-J. *et al.* Unusual Enhancement of Photocurrent by Incorporation of Brönsted Base Thiourea into Electrolyte of Dye-Sensitized Solar Cell. *J. Chem. Phys. C* **114**, 19849-19852 (2010).

26 Ito, S. *et al.* Photovoltaic characterization of dye-sensitized solar cells: effect of device masking on conversion efficiency. *Prog. Photovolt: Res. Appl.* **14**, 589-601, (2006).